E-Article

Individual Specialization and Multihost Epidemics: Disease Spread in Plant-Pollinator Networks

Stephen P. Ellner,[1,*] Wee Hao Ng,[2] and Christopher R. Myers[3]

1. Department of Ecology and Evolutionary Biology, Cornell University, Ithaca, New York 14853; 2. Department of Entomology, Cornell University, Ithaca, New York 14853; 3. Center for Advanced Computing and Laboratory of Atomic and Solid State Physics, Cornell University, Ithaca, New York 14853

Submitted August 15, 2019; Accepted November 14, 2019; Electronically published April 2, 2020

Online enhancements: supplemental PDF, computer scripts.

abstract: Many parasites infect multiple species and persist through a combination of within- and between-species transmission. Multispecies transmission networks are typically constructed at the species level, linking two species if any individuals of those species interact. However, generalist species often consist of specialized individuals that prefer different subsets of available resources, so individual- and species-level contact networks can differ systematically. To explore the epidemiological impacts of host specialization, we build and study a model for pollinator pathogens on plant-pollinator networks, in which individual pollinators have dynamic preferences for different flower species. We find that modeling and analysis that ignore individual host specialization can predict die-off of a disease that is actually strongly persistent and can badly over- or underpredict steady-state disease prevalence. Effects of individual preferences remain substantial whenever mean preference duration exceeds half of the mean time from infection to recovery or death. Similar results hold in a model where hosts foraging in different habitats have different frequencies of contact with an environmental reservoir for the pathogen. Thus, even if all hosts have the same long-run average behavior, dynamic individual differences can profoundly affect disease persistence and prevalence.

Keywords: infectious disease, model, specialization, contact network, plant-pollinator network.

Introduction

Most parasites infect multiple host species (e.g., Fenton et al. 2015; Levi et al. 2016), and pathogen persistence involves spread within and among multiple host species differing in susceptibility and infectiousness, as well as possibly free-living populations in environmental reservoirs. Modeling of multispecies disease systems for forecasting and control is typically based on species-level contact networks and rates (e.g., Holt et al. 2003; Dobson 2004; Zhuang et al. 2013; Fenton et al. 2015). Community interaction networks are typically constructed at the species level or above. For example, a food web will link species (or higher-level taxa) *i* and *j* if any taxon *i* individual eats a taxon *j* individual, and a network describing disease spread among multiple hosts and vectors will link host species *i* and vector species *j* if there are any contacts between two individuals of those species.

However, generalist species in a wide variety of taxa often consist of individuals that are far more specialized with regard to what they eat or where they forage (e.g., Bolnick et al. 2003, 2007; Estes et al. 2003; Woo et al. 2008; Newsome et al. 2009; Vander Zanden et al. 2010; Araújo et al. 2011; Matich et al. 2011; de Lima et al. 2019; Maldonado et al. 2019). Individual diet and foraging specialization may be advantageous if it facilitates development of expertise at detecting or efficiently exploiting a subset of available resources (Tinker et al. 2008; Dukas 2019). Specialized preferences may be labile so that an individual's lifetime niche breadth is much broader than their niche breadth at any one time (e.g., Heinrich 1979; Novak and Tinker 2015; Russell et al. 2017; Szigeti et al. 2019), or they may be long-lasting (e.g., bumblebees' floral preferences can last a month or longer; Heinrich 1976), even passing from parent to offspring (e.g., Estes et al. 2003). However, relatively few studies have quantified the temporal consistency of intraspecific specializations—how often and to what degree individual specializations change (Novak and Tinker 2015).

In this article, we ask how predictions of pathogen persistence or extinction, determined by the pathogen reproduction number R_0, and of steady-state prevalence for an endemic disease are affected if the modeling and analysis ignore the existence of individual-level specialized food or habitat preferences, either transient or long-lasting. The answer, in brief, is "a whole lot."

* Corresponding author; email: spe2@cornell.edu.

ORCIDs: Ellner, https://orcid.org/0000-0002-8351-9734; Myers, https://orcid.org/0000-0002-2294-2416.

Am. Nat. 2020. Vol. 195, pp. E118–E131.
DOI: 10.1086/708272

The motivation and empirical context for this study is disease spread in communities of pollinating insects, especially bees, and the flowers they visit to collect nectar and pollen. Populations of many bees and other pollinators are in decline, and a variety of emerging or reemergent pathogens are a likely contributing factor (Goulson et al. 2015). For example, deformed wing virus is a major threat to honeybees worldwide (McMahon et al. 2016; Wilfert et al. 2016), with recent evidence of spillover to wild bumblebees (Alger et al. 2019; Manley et al. 2019). The trypanosome *Crithidia bombi* is a widespread virulent parasite in multiple bumblebee species (Koch and Schmid-Hempel 2011), and virulent fungal pathogens, such as *Ascosphaera* spp., attack many wild megachilid bees, such as *Osmia* spp. (Evison et al. 2012; Evison and Jensen 2018). Many pathogens are shared among multiple bee species (Goulson 2009; Evison et al. 2012; Ravoet et al. 2014; McMahon et al. 2015). For the pathogens that we are studying empirically and model here (including *Crithidia*), flowers act as the disease vectors. Transmission among foraging insect hosts is primarily fecal-oral, occurring through shared use of flowers, where uninfected insects can encounter pathogen-laden feces deposited recently by an infected host of the same or another species (Durrer and Schmid-Hempel 1994; Ruiz-Gonzalez and Brown 2006; Singh et al. 2010; McArt et al. 2014; Graystock et al. 2015; Figueroa et al. 2019).

It has long been known that individual pollinators are often more specialized than their species as a whole, visiting within some time window only or primarily a small subset of the flower species visited frequently by their species. Heinrich (1979) referred to this as "majoring" in bumblebees. Szigeti et al. (2019, p. 649) similarly described foraging butterflies as "sequential specialist, i.e. short-term specialist and long-term generalist," because preferences were always narrow but changed over individuals' lifetimes. Individual pollinators may even specialize on a subset of individuals within the species that they visit (Dupont et al. 2011, 2014). In a montane plant-pollinator network, Tur et al. (2014) found that individual pollinators visited on average only about half of the plant species to which their species was linked in the species-level contact network, implying that the species-level network would exaggerate the potential for pollen flow.

The same is likely true for spread of an endemic disease across a network, analogous to how spatial population structure typically impedes disease spread, such that a within-group pathogen reproduction number R_0 well above one is generally required for substantial cross-group infection (Cross et al. 2005, 2007). However, we hypothesized that individual-level specialization would have the opposite effect on disease establishment and persistence. Hosts currently specializing on flowers that they readily infect and acquire infection from would constitute a subnetwork where the disease could persist, and from those hosts and flowers it could spill over to other components of the network.

To test this hypothesis, we construct and study a simple model for pathogen transmission in a pollination network in which pollinator host individuals are sequential specialists, visiting only one flower species for a block of time and then switching to another such species at a characteristic switching rate. Viewed broadly, our model is a dynamic contact network with heterogeneous individuals (e.g., Fefferman and Ng 2007; Volz and Meyers 2007; Holme and Saramaki 2012; Valverde et al. 2016; White et al. 2017, 2018) and with subgroup structure, analogous in some ways to spatial structure, resulting from species differing in their average contact rates with other species. However, the distinctive structure and rewiring patterns resulting from sequential specialization lead to distinctive and unexpected properties. The key feature is that instead of ongoing gain and loss of single links in the network, whenever a host changes foraging specialization they simultaneously break all their links and immediately replace them with new and different links, all with a single flower species different from the one previously visited.

Our goal is to characterize how the pathogen reproduction number R_0 and long-term disease prevalence are affected by the existence of individual-level sequential specialization and by the temporal constancy of specialized preferences. Across a wide range of parameter values and contact network structures, we find that the effects of individual specialization can be extremely large. A model ignoring sequential specialization can be wildly inaccurate about whether a pathogen can persist, typically (but not always) underestimating the potential for disease persistence.

For specificity we refer to hosts as bees, but the model is not bee specific or even pollinator specific (and would be inappropriate for social bees, as it omits direct transmission between hosts). Moreover, we show (as outlined in "Discussion") that our key findings hold in a very different model, inspired by Wilber et al. (2019), where individual-level foraging preferences entail different levels of contact with an environmental reservoir for the pathogen. The fundamental mechanism is the same in both cases, persistence of the disease in the subnetwork of hosts whose current specializations make them good infectors and/or infectees.

Computer scripts to replicate all results and figures in this article are provided online in the supplemental material.[1]

Methods: The General Model

Our starting point is the Truitt et al. (2019) model for a pathogen spreading among multiple species of flowers

1. Code that appears in *The American Naturalist* is provided as a convenience to readers. It has not necessarily been tested as part of peer review.

and pollinator hosts in a plant-pollinator network, with the contact network structured by plant and pollinator traits. As in that model, we assume that the disease is susceptible-infected-susceptible (SIS) in both pollinators and flowers: individuals that recover from infection are again susceptible and unchanged by having been infected. We extend the model of Truitt and colleagues by including dynamically changing foraging preferences among pollinator hosts of the same species. Model notation is summarized in table 1. Truitt et al. (2019) conducted an extensive literature survey to estimate parameters and parameter ranges for native bees in old-field communities in upstate New York (their table 1), which we use here in several of the numerical examples below.

We consider a network of Q bee species foraging on at least two out of K flower species. During any brief period, however, each individual bee visits only one flower species; a bee currently visiting flower species k will be called a type k bee. Apart from current flower preference, all bees in a species are identical. Let $\sigma a_{q,k,j}$ denote the rate at which a type j bee in species q switches to type $k \neq j$, and define $-\sigma a_{q,j,j}$ to be the total rate at which a species q, type j bee switches to some other type, where

$$a_{q,j,j} = -\sum_{k \neq j} a_{q,k,j}. \tag{1}$$

We assume that $|a_{q,j,j}| \approx 1$ for all bee and flower species, so that σ measures the total rate of switching, which we can adjust to study how outcomes such as disease persistence and prevalence depend on switching rate. The long-term average preference distribution of a species q bee, which we denote by $\eta_{q,k}$, $k = 1, 2, \ldots, K$, is given by the equilibrium of the switching dynamic $d\vec{\eta}_q/dt = \sigma \mathbf{a}_q \vec{\eta}_q$ on the space of discrete probability distributions, where $\mathbf{a}_q$ is the matrix with entries $a_{q,k,j}$.

In numerical studies, we considered three preference structures. The first was nearly uniform preferences $\eta_{q,k} \approx 1/K$ resulting from small random perturbations of completely random switching $a_{q,k,j} = 1/(K-1)$ for all $k \neq j$. The other two were trait-based preferences, modeling patterns frequently observed empirically in pollination networks (Truitt et al. 2019). Host and flower species are assigned evenly spaced trait values on the interval [0,1]. In "trait matching," the traits are interpreted as scaled size measures (e.g., tongue length and corolla tube length), and hosts preferentially switch to flowers with traits most similar to their own. In "nested" preferences (Truitt et al. 2019), x and y are interpreted as choosiness and attractiveness, respectively. All hosts preferentially switch to more attractive flowers, with choosier hosts having a stronger bias toward more attractive flowers. The strength of trait-based preferences is controlled by parameters s and n, which determine how strongly pollinators prefer similar-sized (trait matching) or more attractive (nested) flowers. In appendix S1 (apps. S1–S9 are available online), we give the formulas for these preference structures and graph

Table 1: Parameters or parameter combinations for the rescaled model (eq. [4]) and their definitions

Parameter	Definition or formula	Units
N_k	Total population of species k flowers	flowers or inflorescences
M_q	Total population of species q bees at the disease-free equilibrium	individuals
b_q	Total birth rate of bees	bees/day
$\alpha_{q,k}$	Transmission rate from infected bee to noncontaminated flower	day^{-1}
$\beta_{q,k}$	Transmission rate from contaminated flower to susceptible bee	day^{-1}
γ_q	Bee rate of recovery from infection	day^{-1}
μ_q	Death rate of susceptible bees	day^{-1}
ν_q	Additional death rate of infected bees	day^{-1}
ζ_k	Flower rate of recovery from infection	day^{-1}
σ	Parameter controlling the overall rate of preference switching	proportion (unitless)
$a_{q,k,j}$	Rate of bee preference switching from flower species j to k, $k \neq j$ for bee species q when $\sigma = 1$; see equation (1) for $k = j$	day^{-1}
$\mathbf{a}_q$	Switching matrix for bee species q, with (k,j) entry $a_{q,k,j}$	day^{-1}
$\eta_{q,k}$	Equilibrium fraction of time that a species q bee is specialized on species k flowers	proportion (unitless)
$R_{0,q,k}$	$(\eta_{q,k}\alpha_{q,k}\beta_{q,k})\zeta_k^{-1}(\gamma_q + \mu_q + \nu_q)^{-1}$	proportion (unitless)
$\boldsymbol{\alpha}_q$	$\mathcal{D}(\alpha_{q,1}, \alpha_{q,2}, \ldots, \alpha_{q,K})$	day^{-1}
$\tilde{\boldsymbol{\beta}}_q$	$\mathcal{D}(\tilde{\beta}_{q,1}, \tilde{\beta}_{q,2}, \ldots, \tilde{\beta}_{q,K})$, where $\tilde{\beta}_{q,k} = \eta_{q,k}\beta_{q,k}$	day^{-1}
$\mathbf{Y}$	$-\mathcal{D}(\zeta_1, \zeta_2, \ldots, \zeta_K)$	day^{-1}
$\mathbf{X}_q(\sigma)$	$-(\gamma_q + \mu_q + \nu_q)\mathbf{I}_K + \sigma\mathbf{a}_q$, where $\mathbf{I}_K$ is the $K \times K$ identity matrix	day^{-1}

Note: Subscripts k and q indicate parameters that vary among flower or bee species, respectively. $\mathcal{D}(\cdot)$ indicates a diagonal matrix with entries $\cdot$ on the diagonal. Units correspond to table 1 in Truitt et al. (2019), which gives estimates and ranges for many of the parameters for old-field communities in upstate New York.

some examples (fig. S1; figs. S1–S7 are available online). All three preference structures are irreducible, so $\eta_{q,k}$ is well defined and unique.

We assume that each flower species k has a constant number of individuals, N_k. For bees, we include demographic processes so that infection can affect mortality. We assume a time-invariant total birth rate b_q (bees/time) for species q, with all newborns uninfected. We assume that natural mortality μ_q and additional mortality of infected bees ν_q vary across bee species but are time invariant and in particular are not affected by the bee's current foraging preference. Define $S_{q,k}$ as the number of bees of species q and type k that are susceptible, $I_{q,k}$ as the number of bees of species q and type k that are infected, U_k as the number of flowers of species k that are pathogen-free (uncontaminated), and C_k as the number of flowers of species k that are contaminated with pathogens. A susceptible species q, type k bee is assumed to become infected through foraging on contaminated flowers at rate $\beta_{q,k}C_k/N_k$. The value of $\beta_{q,k}$ combines the rate of flower visitation by each type k bee and the chance of infection given visitation to a contaminated flower. Both of those may vary across flower species. The factor C_k/N_k assumes that bees visit flowers of their preferred species at random, without regard to whether they are contaminated.

Similarly, each infected species q, type k bee contaminates uncontaminated species k flowers at total rate $\alpha_{q,k}U_k/N_k$, where $\alpha_{q,k}$ combines the per-bee visitation rate to species k flowers with the chance of causing contamination on each such visit.

The disease is assumed to be SIS: once a bee or flower clears infection, it becomes susceptible again. An infected species q bee recovers at rate γ_q (independent of current foraging preference), and a contaminated flower of species k becomes pathogen-free at rate ζ_k.

To complete the model, we need to specify the type (foraging preference) distributions of newborn bees in each species. We assume that the fractions at birth equal the steady-state fractions $\eta_{q,k}$ resulting from the switching rates. Thus, species q bees of type k are born at rates $\eta_{q,k}b_q$. The reason for this assumption (besides avoiding additional parameters) is that it is necessary to have a controlled experiment for the effect of bee specialization—that is, for effects of changing the value of σ. With this assumption, all σ values produce the same species-level link strengths in the absence of disease—that is, the same values for the overall frequency of visits by species q bees to species k flowers. Different values of σ then result in different individual-level behaviors that all produce the same species-level network. Otherwise, different σ values would produce different visitation rates in the absence of disease, which would be confounded with the effect of switching rate per se.

These assumptions give the following dynamic equations:

$$\begin{aligned}
\frac{dS_{q,k}}{dt} &= b_q\eta_{q,k} + \gamma_q I_{q,k} - \beta_{q,k}S_{q,k}C_k/N_k - \mu_q S_{q,k} \\
&\quad + \sigma\sum_{j=1}^{K} a_{q,k,j}S_{q,j}, \\
\frac{dI_{q,k}}{dt} &= \beta_{q,k}S_{q,k}C_k/N_k - (\gamma_q + \mu_q + \nu_q)I_{q,k} + \sigma\sum_{j=1}^{K} a_{q,k,j}I_{q,j}, \\
\frac{dC_k}{dt} &= \left(\frac{U_k}{N_k}\right)\sum_{q=1}^{Q}\alpha_{q,k}I_{q,k} - \zeta_k C_k, \quad \text{where } U_k = N_k - C_k.
\end{aligned} \tag{2}$$

As above, $\alpha_{q,k}$ and $\beta_{q,k}$ reflect the net effect of flower visitation and pathogen transmission rates for a species q bee currently specializing on species k flowers.

We can reduce the parameter count by scaling bee abundance relative to their disease-free steady-state abundance $M_q \equiv b_q/\mu_q$ and flowers relative to their total abundance N_k. However, we do not rescale time because little is gained by doing so. Defining

$$\begin{aligned}
s_{q,k} &= S_{q,k}/M_q, y_{q,k} = I_{q,k}/M_q, c_k = C_k/N_k, \tilde{\alpha}_{q,k} \\
&= M_q\alpha_{q,k}/N_k,
\end{aligned} \tag{3}$$

the rescaled model is

$$\begin{aligned}
\frac{ds_{q,k}}{dt} &= \mu_q\eta_{q,k} + \gamma_q y_{q,k} - \beta_{q,k}s_{q,k}c_k - \mu_q s_{q,k} + \sigma\sum_{j=1}^{K} a_{q,k,j}s_{q,j}, \\
\frac{dy_{q,k}}{dt} &= \beta_{q,k}s_{q,k}c_k - (\gamma_q + \mu_q + \nu_q)y_{q,k} + \sigma\sum_{j=1}^{K} a_{q,k,j}y_{q,j}, \\
\frac{dc_k}{dt} &= (1 - c_k)\sum_{q=1}^{Q}\tilde{\alpha}_{q,k}y_{q,k} - \zeta_k c_k.
\end{aligned} \tag{4}$$

Henceforth, we will always work with the rescaled model, and for clarity we write α in place of $\tilde{\alpha}$. Two parameter combinations that arise repeatedly are

$$\hat{\beta}_{q,k} = \beta_{q,k}/\zeta_k, \quad \hat{\alpha}_{q,k} = \alpha_{q,k}/(\gamma_q + \mu_q + \nu_q). \tag{5}$$

These are both measures of "lifetime infectivity": per capita infectivity (to a particular kind of potential infectee) multiplied by the average time to recovery for flowers and the average time to death or recovery for bees.

Results: The No-Switching and Rapid-Switching Limits

The goal of our model analysis is to discover how model predictions depend on whether the pollinator hosts are generalists or "sequential specialists" with preferences that are always narrow but change over time to eventually

(if they live long enough) encompass the full niche breadth of their species (Szigeti et al. 2019; see also other studies mentioned in the introduction).

In this section, we begin our study by asking how the pathogen's reproduction number R_0 and steady-state disease prevalence in bees vary as a function of the switching rate parameter σ. As $\sigma \to 0$, individual bees spend a greater and greater fraction of their life foraging on their initially preferred flower species, and when $\sigma = 0$, they spend their whole life specialized on that one species. As $\sigma \to \infty$, each bee is effectively nonspecialized.

The reproduction number R_0 is the largest eigenvalue of the next-generation matrix (NGM), which describes the linearized dynamics for the infected subsystem at the disease-free equilibrium (e.g., Diekmann et al. 2010). For our model, it is convenient to define one generation as bee-to-bee transmission mediated by flowers or, equivalently, flower-to-flower transmission mediated by bees.

When there is no switching ($\sigma = 0$), the system reduces to a collection of unconnected networks, each consisting of one flower species and the bees in any species that visit it. The value of R_0 for the system as a whole is the maximum R_0 for any of the unconnected subnetworks (because the eigenvalues of a block-diagonal matrix are the eigenvalues of the blocks). Importantly, this maximum subnetwork R_0 is also the limiting value of R_0 for the full system as $\sigma \to 0$, because eigenvalues are a continuous function of matrix entries (e.g., Horn and Johnson 1985, app. D), and hence approximates the full-system R_0 when σ is very small.

Because there is only one flower species in each subnetwork when $\sigma = 0$, the flower-to-flower NGM is 1×1, and it can be computed directly by considering flower-to-flower transmission mediated by all bees. Each species k flower remains contaminated for average time $1/\zeta_k$, infecting $\beta_{q,k}\eta_{q,k}$ bees of species q per unit of time, which are all type k. Each species q bee of type k remains infected for average time $1/(\gamma_q + \mu_q + \nu_q)$, contaminating $\alpha_{q,k}$ flowers of species k per unit of time. The value of R_0 for the flower species k subnetwork is therefore (in terms of rescaled model parameters)

$$R_{0,k} = \sum_{q=1}^{Q} R_{0,q,k}, \quad \text{where } R_{0,q,k} = \frac{\eta_{q,k}\alpha_{q,k}\beta_{q,k}}{\zeta_k(\gamma_q + \mu_q + \nu_q)} = \eta_{q,k}\hat{\alpha}_{q,k}\hat{\beta}_{q,k}. \tag{6}$$

The value of R_0 for the community as a whole is $R_0(0) = \max_k R_{0,k}$.

The system also simplifies considerably in the rapid-switching limit $\sigma \to \infty$. In that limit, all bees in a species are equivalent because the infected fraction is the same for all types. Bee species q thus collapses to a single type that is constantly allocating fraction $\eta_{q,k}$ of foraging time to flower species k. The value of R_0 can then be derived from the $Q \times Q$ matrix describing one "generation" of bee-to-bee transmission mediated by flowers. Each species n bee remains infected for time $(\gamma_n + \mu_n + \nu_n)^{-1}$ and infects $\eta_{n,k}\alpha_{n,k}/(\gamma_n + \mu_n + \nu_n) = \eta_{n,k}\hat{\alpha}_{n,k}$ flowers of species k. Each species k flower remains infected for time $1/\zeta_k$ and infects $\eta_{m,k}\beta_{m,k}/\zeta_k = \eta_{m,k}\hat{\beta}_{m,k}$ bees of species m. Thus, the $Q \times Q$ matrix $\mathbf{Q}^\infty$ with entries

$$\mathbf{Q}^\infty_{m,n} = \sum_{k=1}^{K} \eta_{n,k}\hat{\alpha}_{n,k}\eta_{m,k}\hat{\beta}_{m,k} \tag{7}$$

is the bee-to-bee transmission matrix, whose largest eigenvalue is the pathogen reproduction number $R_0(\infty)$.

Numerical solutions of the full model with randomly generated parameters and $\sigma \ll 1$ or $\sigma \gg 1$ confirm that the values of $R_0(0)$ and $R_0(\infty)$ correctly predict whether the disease persists, in both the slow- and the rapid-switching limits (fig. S5).

In numerical experiments with randomly generated parameters (for examples with each of the three preference structures, see figs. 1 and S2), we found that $R_0(0)$ was larger than $R_0(\infty)$, often by a wide margin. Parameters such that $R_0(\infty) < 1$, implying that the disease could not persist with rapid preference switching, could have $R_0(0)$ values as high as 5 or 6. In those cases, if individual foraging preferences change slowly, modeling and analysis that failed to recognize the existence of heterogeneous individual preferences would predict die-off of a pathogen that is in fact strongly persistent.

The situation is more complicated regarding steady-state disease prevalence. For a given R_0, steady-state disease prevalence is generally higher with rapid switching than with slow switching (fig. S5), and this can counteract the effect of switching rate on R_0. When the pathogen is unable or barely able to persist with rapid switching, its prevalence at a low switching rate may be considerably higher (e.g., nearly 10% rather than 3%; figs. 2, S3). In contrast, if the pathogen is able to persist at moderate or high abundance even when switching is rapid, its prevalence at a low switching rate could be lower by a factor of two. Thus, if individual preferences are permanent or change slowly, an analysis ignoring this heterogeneity could substantially over- or underpredict the steady-state disease prevalence.

But is it actually true that $R_0(\infty)$ is always less than $R_0(0)$? In the case of $Q = 1$ bee species, the mathematics simplifies considerably: $R_{0,k}$ reduces to (dropping the q index) $R_{0,k} = \eta_k\hat{\alpha}_k\hat{\beta}_k$, and the matrix $\mathbf{Q}^\infty$ reduces to a single number. Therefore,

$$R_0(\infty) = \mathbf{Q}^\infty = \sum_{k=1}^{K} \eta_k^2\hat{\alpha}_k\hat{\beta}_k \le \sum_{k=1}^{K} \eta_k \max_j R_{0,j} = R_0(0), \tag{8}$$

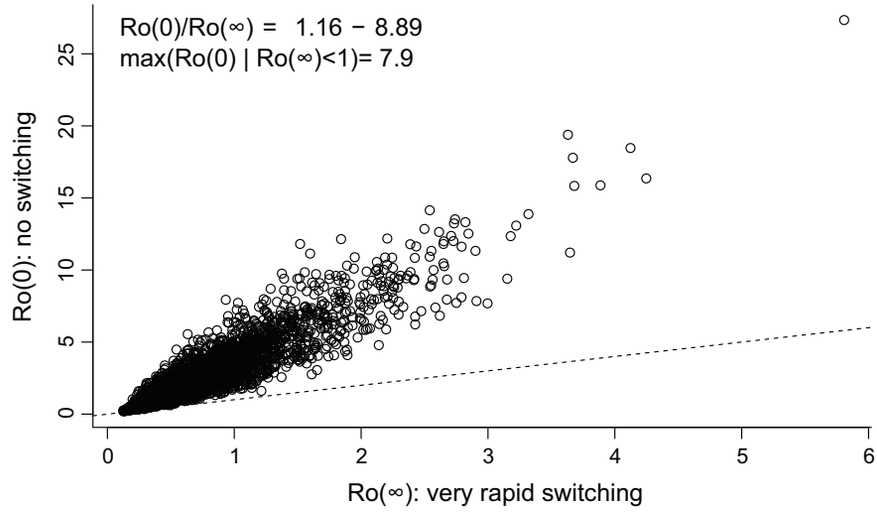

Figure 1: Comparison of $R_0(0)$ (no switching) versus $R_0(\infty)$ (very rapid switching) for 2,500 randomly generated parameter values, with $Q = 15$, $K = 10$. Baseline parameters for all species and species pairs $\zeta = 2$, $\gamma = 0.1$, $\mu = 0.03$, $\nu = 0.02$, $\alpha = 0.01$, $\beta = 9$, taken from table 1 of Truitt et al. (2019) except that β was chosen to give $R_0 \approx 1$ at the baseline values. The expression $\max(R_0(0)|R_0(\infty) < 1)$ is the largest $R_0(0)$ for which the corresponding $R_0(\infty)$ value is <1 so that a model ignoring individual specialization would predict pathogen die-off. Parameter sets were generated by multiplying the baseline value (for each species or pair) by independent Uniform(0.05, 1.95) random numbers. Preferences $\eta_{q,k}$ resulted from a nested network with $n = 3$. Corresponding results for random and trait-matching networks are shown in figure S2. This figure was generated by R script R0_and_mixing.R.

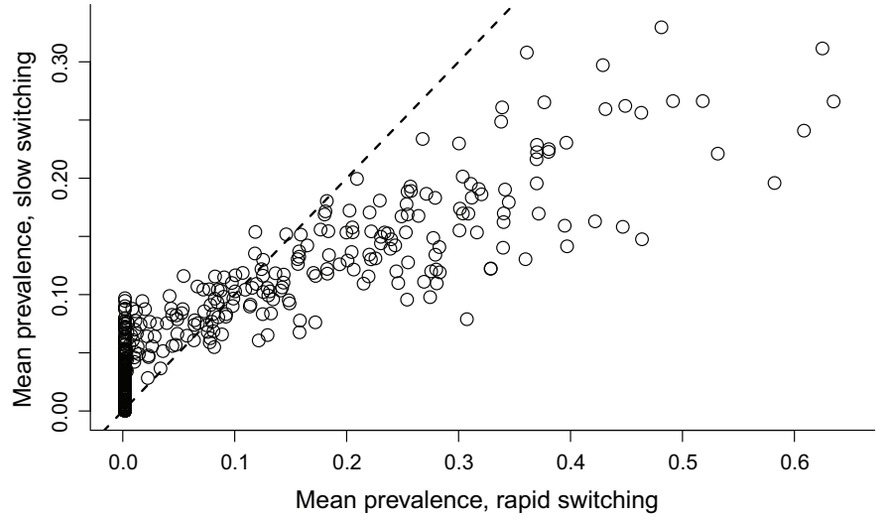

Figure 2: Comparison of steady-state disease prevalence in bees (infected bees/total bees including all species) with $\sigma = 0.01$ (slow switching) versus $\sigma = 100$ (rapid switching) for 500 randomly generated parameter values, with $Q = 5$, $K = 10$. The dashed line is the 1:1 line. Baseline parameters for all species and species pairs were $\zeta = 0.2$, $\gamma = \mu = 0.15$, $\alpha = 0.05$, $\beta = 2$. This baseline differs from figure 1 to obtain a wider range of prevalence values, and very similar results (not shown) were obtained without exception for other choices of baseline. Parameter sets were generated as in figure 1. Simulations were initialized with disease prevalence of 2.5% in all flower species and 0.5% in all bee species and run to time $t = 5{,}000$; plotting trajectories of disease prevalence over time (results not shown) confirmed that $t = 5{,}000$ is sufficient for disease prevalence to reach steady state. Preferences $\eta_{q,k}$ resulted from a nested network with $n = 3$. Corresponding results for random and trait-matching networks are shown in figure S3. This figure was generated by R script Prevalence_and_mixing.R.

with equality only when $R_{0,k}$ is the same for all k with $\eta_k > 0$. In other words, apart from that exceptional situation, for $Q = 1$ very slow mixing always leads to greater disease persistence than very rapid mixing. For the simplest such case—one bee species and two flower species—it is moreover the case that $R_0(\sigma)$ is a monotonically decreasing function of σ (see app. S3): faster preference switching always makes a disease outbreak less likely to occur.

To our surprise, we found that this pattern does not always hold with two or more pollinator species. Generating random parameter sets, $R_0(\infty) > R_0(0)$ is always infrequent but is least rare when there are few flower species (figs. 3, S4; simulation details are in app. S4). The frequency of these exceptional parameter sets depends weakly on the number of bee species but decreases quickly as the number of flower species increases. However, even for $K = 10$ flower species and $Q = 10$ bee species, there is a minute fraction of exceptional parameter sets drawn from lognormal distributions (<0.1%; see script ConjectureFail.R).

When Does Rapid Switching Increase R_0?

To see when R_0 is increased by rapid switching (or equivalently, by absence of individual-level specialization), we first consider the simplest case: two bee and two flower species ($Q = K = 2$). Here we present the main results; derivations are in appendix S5.

In the no-switching limit, the two-generation R_0 (eq. [6]) is $R_0(0) = \max_k(R_{0,1,k} + R_{0,2,k})$. In the rapid-switching limit, we find in appendix S5 that

$$R_0(\infty) = \frac{1}{2}\left[\bar{R}_0 + \sqrt{\bar{R}_0^2 + 4\Delta}\right], \tag{9}$$

where

$$\begin{aligned}\bar{R}_0 &= \eta_{1,1}R_{0,1,1} + \eta_{1,2}R_{0,1,2} + \eta_{2,1}R_{0,2,1} + \eta_{2,2}R_{0,2,2},\\ \Delta &= \eta_{1,1}\eta_{1,2}\eta_{2,1}\eta_{2,2}(\hat{\alpha}_{1,1}\hat{\alpha}_{2,2}\hat{\beta}_{2,1}\hat{\beta}_{1,2} + \hat{\alpha}_{1,2}\hat{\alpha}_{2,1}\hat{\beta}_{1,1}\hat{\beta}_{2,2})\\ &\quad - \eta_{1,1}\eta_{2,2}R_{0,1,1}R_{0,2,2} - \eta_{1,2}\eta_{2,1}R_{0,1,2}R_{0,2,1}.\end{aligned} \tag{10}$$

Because $\bar{R}_0 \le R_0(0)$, $R_0(\infty)$ can exceed $R_0(0)$ only if the contribution from Δ is positive and large. For example, the first term in Δ will be very large if $\hat{\alpha}_{1,1}$, $\hat{\alpha}_{2,2}$, $\hat{\beta}_{2,1}$, and $\hat{\beta}_{1,2}$ are all large, and if $\hat{\beta}_{1,1}$, $\hat{\beta}_{2,2}$, $\hat{\alpha}_{2,1}$, and $\hat{\alpha}_{1,2}$ are all very small, then all of the $R_{0,q,k}$ are small and hence $R_0(0)$ is small.

The biological interpretation of this situation is that in each bee-flower pair, transmission from bee to flower ($\hat{\alpha}_{q,k}$) or from flower to bee ($\hat{\beta}_{q,k}$) is small, so the disease cannot persist by transmitting back and forth between any one bee-flower pair. See figure 4*A* for an example. Effective transmission pathways in this network (i.e., pathways not including any narrow blue arrows) must include preference switching by hosts, which can create new and highly effective transmission pathways (fig. 4*B*) if switching is rapid.

This mechanism is impossible with only one species ($Q = 1$) because each flower species interacts with only one bee type. A pathway created by switching can be effective only if some flower species has high transmission in both directions with a bee type that visits it. But in that case, disease persistence is most likely when those bees stick to those high transmission links. Moreover, the structure of the network can preclude formation of effective transmission pathways through switching, even with more than one bee species, as illustrated in figure 4*C*, 4*D*. To create an effective pathway in that network, bees would have to change species identity (e.g., $\text{Bee}_{1,1}$ to $\text{Bee}_{2,1}$), which is impossible. Thus, a network where each bee-flower pair has

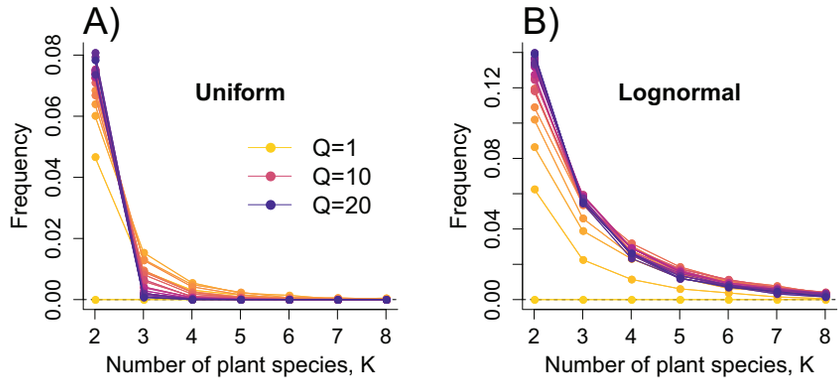

Figure 3: Frequency of the exceptional parameter sets giving $R_0(\infty) > R_0(0)$ in randomly generated parameter sets for varying numbers of plant species in the transmission network. Parameters were generated by random draws from uniform distributions in *A* and from lognormal distributions in *B*. For details of the random parameter generation, see appendix S4. Preferences $\eta_{q,k}$ resulted from a nested network with $n = 5$. Corresponding results for random and trait-matching networks are shown in figure S4. This figure was generated by R script ConjectureFail.R.

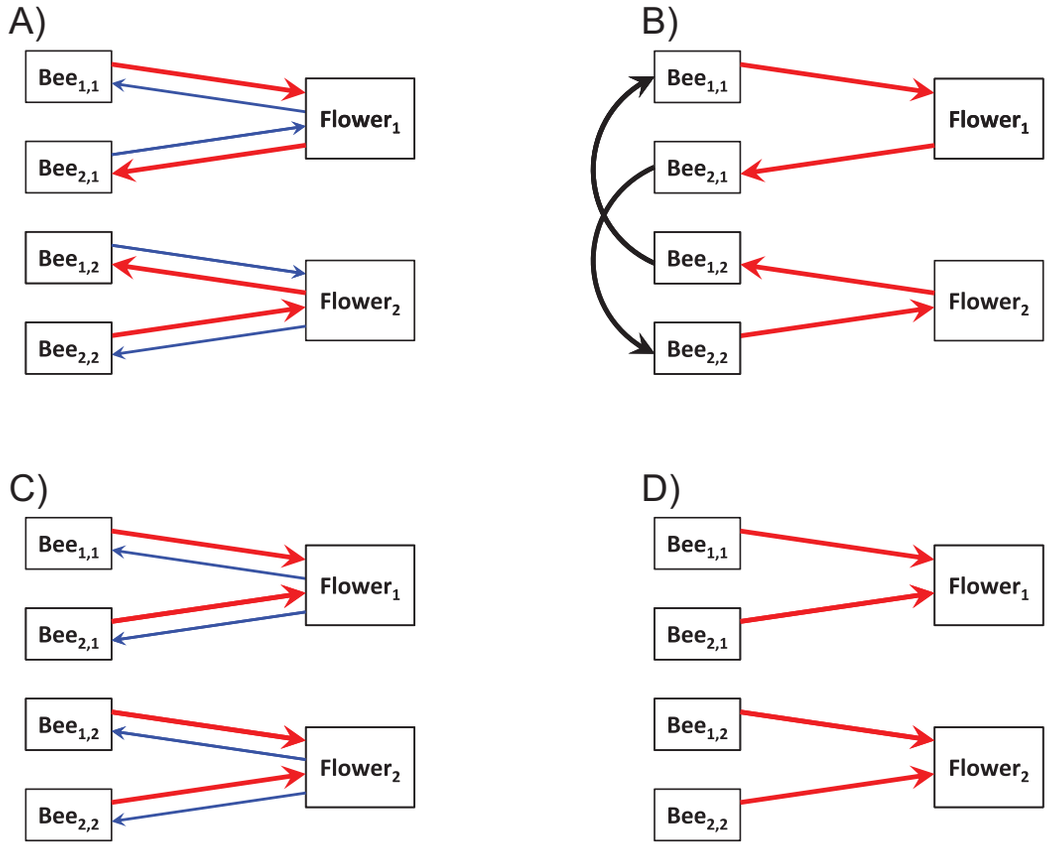

Figure 4: Illustration of how $R_0(\infty)$ can be larger than $R_0(0)$ for some exceptional parameter sets, with two bee and two flower species. *A*, Red (wide) and blue (narrow) arrows indicate high and low transmission rate parameters, respectively. In the absence of switching, any transmission pathway from a species back to itself must traverse an equal number of red and blue arrows. *B*, Rapid switching (black curved arrows) creates a transmission pathway through the whole community that traverses only red arrows and fast black switching arrows. Such a pathway has to utilize both bee species and hence does not exist for $Q = 1$ bee species. Provided that none of the equilibrium preferences $\eta_{q,k}$ are too small, this will lead to $R_0(\infty) > R_0(0)$. *C*, *D*, Example illustrating that poor back-and-forth transmission in all bee-flower pairs is not sufficient for a parameter set to be exceptional. Because every path from a flower species to itself traverses red and blue arrows, preference switching cannot create any pathway from a species to itself that traverses only high-transmission arrows.

poor transmission in at least one direction is necessary, but not sufficient, for faster switching to increase R_0.

These general properties of small networks are supported by simulations with larger networks (fig. S6). Specifically, exceptional parameter sets were characterized by low values of $\max_{q,k}(\hat{\alpha}_{q,k}\hat{\beta}_{q,k})$. Low values indicate that high transmission in one direction is always accompanied by low transmission in the other, so no bee-flower pair can maintain the pathogen by passing it back and forth between themselves. Preference switching may then promote pathogen persistence, but it also might not, depending on other features of the network.

Results: Intermediate Switching Rates

So far, we have been contrasting the extreme cases of very slow switching and very rapid switching. In the former limit, within-species foraging specializations are fixed for life; in the latter, specializations change so fast that individuals are really generalists with no within-species variation. We now explore how R_0 varies in between those limits, when individuals really are sequential specialists. As before, we consider flower-to-flower transmission mediated by bees (or equivalently, bee-to-bee transmission mediated by flowers) as a single "generation" for calculating R_0 using a next-generation matrix.

In appendix S6, using notation defined in table 1, we show that the flower-to-flower next-generation matrix is

$$\mathbf{Z}(\sigma) = \left(\sum_{q=1}^{Q} \boldsymbol{\alpha}_q \mathbf{X}_q^{-1}(\sigma)\tilde{\boldsymbol{\beta}}_q\right)\mathbf{Y}^{-1}. \tag{11}$$

Both $\tilde{\boldsymbol{\beta}}_q$ and $\boldsymbol{\alpha}_q$ are analogous to the βN component of R_0 in a single-species SIS model. The difference between

them results from scaling the model so that every flower species has abundance one, while species q, type k bees have abundance $\eta_{q,k}$ when disease is absent. Since $\mathbf{Z}(0) = \mathcal{D}(R_{0,1}, R_{0,2}, \ldots, R_{0,k})$, equation (6) is confirmed, and we numerically confirmed that R_0 from $\mathbf{Z}(\sigma)$ agrees with R_0 from equation (7) for large σ (script Check_Z_limits.R).

As $\sigma \to \infty$, $\mathbf{Z}(\sigma)$ converges to the matrix with entries

$$\mathbf{Z}(\infty)_{m,n} = \sum_{q=1}^{Q} \eta_{q,m}\hat{\alpha}_{q,m}\eta_{q,n}\hat{\beta}_{q,n}, \tag{12}$$

analogous to equation (7) (see app. S7). Intuitively, the difference between $\mathbf{Z}(\sigma)$ and $\mathbf{Z}(\infty)$ is that with infinitely fast switching, an infected bee immediately "forgets" which flower species it was visiting when it got infected and visits each flower species according to its long-run average preference $\eta_{q,k}$. With finite switching rate, newly infected bees initially continue to specialize on the flower species that infected them, so on average they spend slightly more time before recovery or death visiting that species, relative to $\eta_{q,k}$, and slightly less time visiting other flowers (we prove this in app. S7).

It is always the case that slow preference switching is less favorable for disease persistence than no switching. Specifically, considering $\mathbf{Z}$ and R_0 as functions of σ, we show in appendix S8 that $R_0'(\sigma) < 0$ at $\sigma = 0$. This general property can be explained heuristically as follows. When $\sigma = 0$, there is no transmission between flower species, so the flower-to-flower NGM is diagonal with diagonal entries $R_{0,k}$, the per-generation rate of pathogen increase in flower species k. The community R_0 is therefore the largest of the $R_{0,k}$ (we call this the "dominant" flower), and the corresponding eigenvector is all zeros except for the entry corresponding to the dominant flower. This says that infection levels in the dominant flower will greatly exceed those in the other flowers, when the pathogen is becoming established. Preference switching thus causes a net loss of pathogen from the dominant flower, slowing the increase of infection in the dominant flower and therefore in the community as a whole.

In contrast, at the rapid-mixing extreme, we have seen that for some exceptional parameter sets $R_0(\sigma)$ is largest at $\sigma = \infty$ and therefore increasing at very large σ. In appendix S7, we show that under certain special conditions $R_0(\sigma) - R_0(\infty)$ is (to leading order in $1/\sigma$) proportional to $\sum_{q=1}^{Q}\mathrm{Cov}(\hat{\alpha}_q, \hat{\beta}_q)$. This aligns with our simulations (fig. S6), in that rapid switching promotes disease persistence only when no bee-flower pair has high transmission in both directions. However, when those special conditions are relaxed, the finite-σ correction to R_0 includes additional terms that can override the impact of $\hat{\alpha}$, $\hat{\beta}$ covariance. This again aligns with the simulation result that negative $\hat{\alpha}$, $\hat{\beta}$ covariance does not necessarily result in R_0 increasing at large σ.

Simulations with randomly generated parameter values (see fig. S7) show that it is uncommon but not extremely rare for $R_0(\sigma)$ to be increasing at large σ (generally <10%, especially for larger K). Thus, disease persistence is generally favored by longer persistence of individual preferences.

When Does Specialization Matter?

The biological relevance of individual specialization in a community depends on how long individual preferences must persist for community properties to differ from the fast-switching limit that is equivalent to no specialization. A useful clue comes from equation (11). Holding everything but σ constant, it is easy to see that the contribution of bee species q to $\mathbf{Z}(\sigma)$ is a function of the ratio $\sigma/(\gamma_q + \mu_q + \nu_q)$. We can interpret this as the ratio between the mean bee infection time $(\gamma_q + \mu_q + \nu_q)^{-1}$ and the characteristic switching time $1/\sigma$.

We therefore predict that there will be a substantial effect of switching when the switching time $1/\sigma$ is comparable to the bee mean infection time, at least when mean infection time is not highly variable from species to species. To test this prediction, we used numerical optimization to find the maximum possible ratio between $R_0(\sigma)$ and $R_0(\infty)$ as a function of model parameters subject to constraints. Without constraints, for any value of σ, the maximum possible ratio is apparently $+\infty$. We therefore imposed the constraint that the ratio between the same parameter for two species or species pairs (e.g., any ratio $\alpha_{q_1,k_1}/\alpha_{q_2,k_2}$) could be at most some number $r > 1$.

The results (fig. 5) support the conjecture. Even when the mean preference duration is only half the mean infection time, the true R_0 for a set of parameters can be three times larger than what it would be without individual specialization when the maximum ratio r equals 4 and nearly six times larger when r equals 10. The effect of specialization decreases sharply with shorter preference durations and saturates with longer preference durations. Numerical values of (true R_0)/(no-specialization R_0) depend on the contact network structure and network size: with few flower species (e.g., $K = 4$), the potential effect of specialization is smaller (results not shown). However, the shape of the relationship is always very similar to that in figure 5 and parallels a plot of "infection loyalty" as a function of relative preference duration. Infection loyalty is the expected fraction of the time until death or recovery that a forager continues to specialize without interruption on the species from which it acquired infection. When infection loyalty is low, the effect of specialization is small. But even when preference durations are substantially shorter

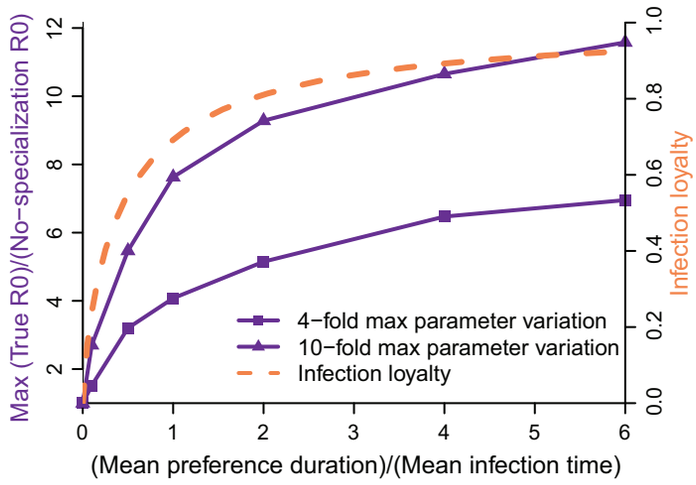

Figure 5: Numerical results showing how the largest possible ratio between the true R_0 for a set of parameters and the R_0 for the same parameters without individual specialization varies with the ratio between mean preference duration $1/\sigma$ and mean infection time (the unweighted average over bee species of $(\gamma_q + \mu_q + \nu_q)^{-1}$). The two solid blue curves (left Y-axis) correspond to two values (4 or 10) for the maximum allowed ratio of values for $\alpha_{q,k}$, $\beta_{q,k}$, ζ_k, or ρ_q across different k and q, within each parameter. Results shown here are for $Q = 8$, $K = 10$, and a trait-matching preference network with $s = 5$. Each maximum ratio was estimated by three iterations of minimizing its inverse with Nelder-Mead search using function optim followed by local quadratic optimization using bobyqa in the minqa R library. The dashed red curve (right Y-axis) is the host "infection loyalty"—the expected fraction of the time from infection until death or recovery that a newly infected host continues to specialize (without interruption) on the flower species that infected it. This figure was generated by R script Maximize_Specialization_Effect.R.

than infection times, infection loyalty can be above 50% and the presence of individual-level specialization can have a large effect on R_0.

With a nested-preference network, the parameter values maximizing the impact of specialization always involved high transmission between the most popular flowers and the most selective foragers and low transmission otherwise. Impact-maximizing parameters for trait-matching networks generally involved a few clusters of bee-flower pairs with high α and β values, but their locations varied unpredictably across optimization runs with different initial parameter guesses.

Discussion

Infectious disease ecologists have long recognized that persistent between-individual variation in contact and/or transmission rates or in location within a contact network can have substantial impacts on the dynamics of infectious disease outbreaks and spread (e.g., Lloyd-Smith et al. 2005; Fenton et al. 2015; Pellis et al. 2015; VanderWaal and Ezenwa 2016; White et al. 2017; Roswell et al. 2019). A classic example is the crucial role played by a small core group, with high contact and infection rates, for the rise and eventual control of gonorrhea incidence rates in the United States (Hethcote and Yorke 1984). Recently, Wilber et al. (2019) found substantial between-individual variation in rates of environmentally mediated ("indirect") bovine tuberculosis transmission among white-tailed deer, raccoon, opossums, and cattle. In multihost communities, between-species variation in contact rates or susceptibility is similarly important (e.g., Dobson 2004; Fenton et al. 2015).

This study demonstrates theoretically that labile specialized preferences for particular resources or habitats can also have major consequences for disease persistence and spread in multispecies disease systems. Specialized preferences are known to be common in insects, fishes, birds, herps, and mammals (e.g., Bolnick et al. 2003; Araújo et al. 2011), and their effects on disease persistence in our models are often not subtle. We found that even when all pollinators in a species have the same lifetime average preferences and niche breadth, the within-species behavioral heterogeneity present at any one moment creates potentially crucial opportunities for a disease to persist in a core group of pollinators focusing their attentions, for the moment, on the subset of flowers with which they have strong back-and-forth transmission links. Another possible analogy is to view specialized preferences as creating "source" and "sink" subnetworks. The source subnetwork consists of pollinator hosts currently specializing on a species of flower with which they have strong pathogen transmission in both directions. Hosts joining the source subnetwork (as a result of a preference switch to one of

those flower species) quickly become infected. Hosts leaving the subnetwork spread the pathogen to other flower species and from there to other hosts, allowing low-level disease presence in sink subnetworks. If preference switching is rapid, joining a source subnetwork is typically too fleeting to have any effect. But when switching occurs on a timescale comparable to disease processes, the effects can be very substantial (figs. 1, 2, 5).

We have chosen to focus on a model for the system that we and our colleagues study empirically, rather than a general model, to take advantage of empirically grounded parameter estimates (Figueroa et al. 2019; Truitt et al. 2019) and because foraging specialization in pollinators is amply documented. Concerns about the generality of our conclusions are therefore natural. We believe that our findings are relevant to any situation where multiple hosts, multiple vectors, or multiple habitats contribute to the persistence of a disease, because the "core group/source subnetwork" phenomenon will always be possible. Any of these kinds of specialization can result in individual-level contact networks being very different from the species average contact network, and it is the former that determine a pathogen's fate and impact. Even when transmission is not a direct consequence of foraging as in our model, foraging preferences are likely to affect where an individual spends its time (as different food items will often be found in distinct locations) and therefore affect its rate of contact with other species and with environmental reservoirs. As one specific example, in appendix S9, we show that our key findings hold in a very different model, inspired by Wilber et al. (2019), where individual foraging preferences entail different levels of contact with an environmental reservoir for the pathogen. We assume that at any one time individuals limit their foraging to one out of m habitat types and occasionally switch preferences. Foraging in one particular habitat type brings them into contact with an environmental reservoir where the pathogen can persist but would die out eventually if it is not sustained by pathogens shed from infected hosts foraging in that habitat. Our key result for this model is that slowly changing preferences can result in R_0 being larger than what it would be, in the absence of foraging preferences, by a factor of up to $\sqrt{m}$ when indirect transmission via the reservoir is highly efficient relative to direct transmission. The ratio over two generations (i.e., m) shows that the effect on R_0 of habitat specialization in this model can easily be comparable to the two-generation effects of pollinator foraging specialization (fig. 5).

Conversely, there are some limitations to our analyses. In both our pollinator model and our environmental reservoir model, we assume that being specialized does not result in a lower total contact rate but simply limits contacts to a subset of the possibilities. In terms of classical foraging theory, we ignore the possibility that specialization will increase search time for preferred flowers or habitats, tacitly assuming that foragers can quickly find and reach their targets even when seeking a less abundant species or habitat. Removing this assumption would be an important direction for extending our models. We have also completely ignored within-species heterogeneity. We expect that within-species heterogeneity in switching rates could have substantial impacts. For bees in particular, we have not considered social bees, where within-colony transmission could have equal or greater importance than flower-mediated transmission.

Our model analyses have taken parameter values as "given" and explored the consequences of individual specialization for projections about disease persistence or prevalence. The consequences may be even greater if the model is first used for inference about parameter values, especially when transmission parameters are fitted to data on infection rates (as is often the case). Suppose, for example, that an empirical estimate for R_0 is derived from an observed increase in prevalence during an outbreak—call it $\hat{R}_0$—and transmission parameters (α or β) in a specialization-free model are chosen to make the model's R_0 equal $\hat{R}_0$. In terms of our analysis, the fitted parameters would ensure that $R_0(\infty) = \hat{R}_0$, whereas in fact they should be chosen so that $R_0(\sigma) = \hat{R}_0$. In a typical situation where $R_0(\infty) < R_0(\sigma)$, the inferred transmission parameters would be biased upward. Disease projections would be based on overestimates of transmission rates and overestimates (by ignoring specialization) of how widely each host would spread the pathogen in the network. Transmission parameter estimates based on prevalence data in an area where the disease is at steady state could be biased in either direction.

Specialization and preferences may sometimes respond predictably to variation in conditions. For example, Tinker et al. (2008) found that diet specialization in sea otters increased when resources were less abundant. Such behavioral adjustments create the potential for resource abundance, or other factors, to indirectly drive variation in disease processes through their effects on individual specialization. Civitello et al. (2018) have investigated the extent to which anthropogenic resource supplementation (in the form of food provisioning, agricultural fertilization, or aquatic nutrient enrichment) can impact infections both directly (e.g., by increasing host population size or altering parasite production within hosts) and indirectly (by altering interactions with other members of the larger ecosystem). These studies suggest possible opportunities for outbreak prediction based on resource availability changes, or control through altering resource availability, in disease systems where individual specialization is an important factor.

Nearly a decade ago, Araújo et al. (2011) were able to review 241 case studies that not only documented but quantified the degree of individual specialization with regard to diet, foraging behavior, habitat choice, and other niche axes. But outside of a few well-studied groups, such as bumblebees and butterflies, there are very few studies where the persistence time of individual preferences has been studied quantitatively (Novak and Tinker 2015). One of our main goals in writing this article was to spur studies on the temporal constancy of specialized preferences: how often do they change, and how much do they change when they do? Such data may be especially hard to get for the pollination systems we have modeled here, because of the challenges of tracking individuals that are small, unpredictable, and able to fly fast. Our results suggest that it could be very worthwhile to develop new individual tracking technologies to make that job easier.

Acknowledgments

We thank Michael Cortez, Laura Figueroa, Scott McArt, Timothy Salazar, two anonymous reviewers, and the editor and associate editor for comments on the manuscript. This work was supported by the National Institute of General Medical Sciences of the National Institutes of Health (award R01GM122062). The content is solely the responsibility of the authors and does not necessarily represent the official views of the National Institutes of Health.

Data and Code Availability

No original data are presented in this paper. All computer scripts supporting the results are provided online in the supplemental material.

Literature Cited

Alger, S. A., P. A. Burnham, H. F. Boncristiani, and A. K. Brody. 2019. RNA virus spillover from managed honeybees (*Apis mellifera*) to wild bumblebees (*Bombus* spp.). PLoS ONE 14:e0217822.

Araújo, M., D. Bolnick, and C. Layman. 2011. The ecological causes of individual specialisation. Ecology Letters 14:948–958.

Bolnick, D. I., R. Svanbäck, M. S. Araujo, and L. Persson. 2007. Comparative support for the niche variation hypothesis that more generalized populations also are more heterogeneous. Proceedings of the National Academy of Sciences of the USA 104:10075–10079.

Bolnick, D. I., R. Svanbäck, J. Fordyce, L. Yang, J. Davis, C. Hulsey, and M. Forister. 2003. The ecology of individuals: incidence and implications of individual specialization. American Naturalist 161:1–28.

Civitello, D., B. Allman, C. Morozumi, and J. Rohr. 2018. Assessing the direct and indirect effects of food provisioning and nutrient enrichment on wildlife infectious disease dynamics. Philosophical Transactions of the Royal Society B 373:20170101.

Cross, P. C., P. L. F. Johnson, J. O. Lloyd-Smith, and W. M. Getz. 2007. Utility of R_0 as a predictor of disease invasion in structured populations. Journal of the Royal Society Interface 4:315–324.

Cross, P. C., J. O. Lloyd-Smith, P. L. F. Johnson, and W. M. Getz. 2005. Duelling timescales of host movement and disease recovery determine invasion of disease in structured populations. Ecology Letters 8:587–595.

de Lima, R. C., V. Franco-Trecu, D. G. Vales, P. Inchausti, E. R. Secchi, and S. Botta. 2019. Individual foraging specialization and sexual niche segregation in South American fur seals. Marine Biology 166:32.

Diekmann, O., J. A. P. Heesterbeek, and M. G. Roberts. 2010. The construction of next-generation matrices for compartmental epidemic models. Journal of the Royal Society Interface 7:873–885.

Dobson, A. 2004. Population dynamics of pathogens with multiple host species. American Naturalist 164(suppl.):S64–S78.

Dukas, R. 2019. Animal expertise: mechanisms, ecology and evolution. Animal Behaviour 147:199–210.

Dupont, Y. L., K. Trøjelsgaard, M. Hagen, M. V. Henriksen, J. M. Olesen, N. M. E. Pedersen, and W. D. Kissling. 2014. Spatial structure of an individual-based plant-pollinator network. Oikos 123:1301–1310.

Dupont, Y. L., K. Trøjelsgaard, and J. M. Olesen. 2011. Scaling down from species to individuals: a flower-visitation network between individual honeybees and thistle plants. Oikos 120:170–177.

Durrer, S., and P. Schmid-Hempel. 1994. Shared use of flowers leads to horizontal pathogen transmission. Proceedings of the Royal Society B 258:299–302.

Estes, J., M. Riedman, M. Staedler, M. Tinker, and B. Lyon. 2003. Individual variation in prey selection by sea otters: patterns, causes and implications. Journal of Animal Ecology 72:144–155.

Evison, S. E. F., and A. B. Jensen. 2018. The biology and prevalence of fungal diseases in managed and wild bees. Current Opinion in Insect Science 26:105–113.

Evison, S. E. F., K. E. Roberts, L. Laurenson, S. Pietravalle, J. Hui, J. C. Biesmeijer, J. E. Smith, G. Budge, and W. O. H. Hughes. 2012. Pervasiveness of parasites in pollinators. PLoS ONE 7: e30641.

Fefferman, N. H., and K. L. Ng. 2007. How disease models in static networks can fail to approximate disease in dynamic networks. Physical Review E 76:031919.

Fenton, A., D. G. Streicker, O. L. Petchey, and A. B. Pedersen. 2015. Are all hosts created equal? partitioning host species contributions to parasite persistence in multihost communities. American Naturalist 186:610–622.

Figueroa, L. L., M. Blinder, C. Grincavitch, A. Jelinek, E. K. Mann, L. A. Merva, L. E. Metz, et al. 2019. Bee pathogen transmission dynamics: deposition, persistence and acquisition on flowers. Proceedings of the Royal Society B 286:20190603.

Goulson, D. 2009. Bumblebees: behaviour, ecology, and conservation. Oxford University Press, New York.

Goulson, D., E. Nicholls, C. Botias, and E. L. Rotheray. 2015. Bee declines driven by combined stress from parasites, pesticides, and lack of flowers. Science 347:1435–1439.

Graystock, P., D. Goulson, and W. O. H. Hughes. 2015. Parasites in bloom: flowers aid dispersal and transmission of pollinator parasites within and between bee species. Proceedings of the Royal Society B 282:20151371.

Heinrich, B. 1976. The foraging specializations of individual bumblebees. Ecological Monographs 46:105–128.

———. 1979. "Majoring" and "minoring" by foraging bumblebees, *Bombus vagans*: an experimental analysis. Ecology 60:245–255.

Hethcote, H., and J. Yorke. 1984. Gonorrhea transmission dynamics and control. Vol. 56. Lecture Notes in Biomathematics. Springer, New York.

Holme, P., and J. Saramaki. 2012. Temporal networks. Physics Reports 519:97–125.

Holt, R. D., A. P. Dobson, M. Begon, R. G. Bowers, and E. M. Schauber. 2003. Parasite establishment in host communities. Ecology Letters 6:837–842.

Horn, R. A., and C. R. Johnson. 1985. Matrix analysis. Cambridge University Press, Cambridge.

Koch, H., and P. Schmid-Hempel. 2011. Socially transmitted gut microbiota protect bumble bees against an intestinal parasite. Proceedings of the National Academy of Sciences of the USA 108:19288–19292.

Levi, T., F. Keesing, R. D. Holt, M. Barfield, and R. S. Ostfeld. 2016. Quantifying dilution and amplification in a community of hosts for tick-borne pathogens. Ecological Applications 26:484–498.

Lloyd-Smith, J., S. Schreiber, P. Kopp, and W. Getz. 2005. Superspreading and the effect of individual variation on disease emergence. Nature 438:355–359.

Maldonado, K., S. D. Newsome, P. Razeto-Barry, J. Manuel Rios, G. Piriz, and P. Sabat. 2019. Individual diet specialisation in sparrows is driven by phenotypic plasticity in traits related to trade-offs in animal performance. Ecology Letters 22:128–137.

Manley, R., B. Temperton, T. Doyle, D. Gates, S. Hedges, M. Boots, and L. Wilfert. 2019. Knock-on community impacts of a novel vector: spillover of emerging DWV-B from *Varroa*-infested honeybees to wild bumblebees. Ecology Letters 22:1306–1315.

Matich, P., M. R. Heithaus, and C. A. Layman. 2011. Contrasting patterns of individual specialization and trophic coupling in two marine apex predators. Journal of Animal Ecology 80:294–305.

McArt, S. H., H. Koch, R. E. Irwin, and L. S. Adler. 2014. Arranging the bouquet of disease: floral traits and the transmission of plant and animal pathogens. Ecology Letters 17:624–636.

McMahon, D. P., M. A. Furst, J. Caspar, P. Theodorou, M. J. F. Brown, and R. J. Paxton. 2015. A sting in the spit: widespread cross-infection of multiple RNA viruses across wild and managed bees. Journal of Animal Ecology 84:615–624.

McMahon, D. P., M. E. Natsopoulou, V. Doublet, M. Fuerst, S. Weging, M. J. F. Brown, A. Gogol-Doering, and R. J. Paxton. 2016. Elevated virulence of an emerging viral genotype as a driver of honeybee loss. Proceedings of the Royal Society B 283:20160811.

Newsome, S. D., M. T. Tinker, D. H. Monson, O. T. Oftedal, K. Ralls, M. M. Staedler, M. L. Fogel, and J. A. Estes. 2009. Using stable isotopes to investigate individual diet specialization in California sea otters (*Enhydra lutris nereis*). Ecology 90:961–974.

Novak, M., and M. T. Tinker. 2015. Timescales alter the inferred strength and temporal consistency of intraspecific diet specialization. Oecologia 178:61–74.

Pellis, L., F. Ball, S. Bansal, K. Eames, T. House, V. Isham, and P. Trapman. 2015. Eight challenges for network epidemic models. Epidemics 10:58–62.

Ravoet, J., L. D. Smet, I. Meeus, G. Smagghe, T. Wenseleers, and D. C. de Graaf. 2014. Widespread occurrence of honey bee pathogens in solitary bees. Journal of Invertebrate Pathology 122:55–58.

Roswell, M., J. Dushoff, and R. Winfree. 2019. Male and female bees show large differences in floral preference. PLoS ONE 14:1–18.

Ruiz-Gonzalez, M. X., and M. J. F. Brown. 2006. Honey bee and bumblebee trypanosomatids: specificity and potential for transmission. Ecological Entomology 31:616–622.

Russell, A. L., S. J. Morrison, E. H. Moschonas, and D. R. Papaj. 2017. Patterns of pollen and nectar foraging specialization by bumblebees over multiple timescales using RFID. Scientific Reports 7:42448.

Singh, R., A. L. Levitt, E. G. Rajotte, E. C. Holmes, N. Ostiguy, D. Vanengelsdorp, W. I. Lipkin, C. W. Depamphilis, A. L. Toth, and D. L. Cox-Foster. 2010. RNA viruses in hymenopteran pollinators: evidence of inter-taxa virus transmission via pollen and potential impact on non-*Apis* hymenopteran species. PLoS ONE 5:e14357.

Szigeti, V., A. Kőrösi, A. Harnos, and J. Kis. 2019. Lifelong foraging and individual specialisation are influenced by temporal changes of resource availability. Oikos 128:649–658.

Tinker, M. T., G. Bentall, and J. A. Estes. 2008. Food limitation leads to behavioral diversification and dietary specialization in sea otters. Proceedings of the National Academy of Sciences of the USA 105:560–565.

Truitt, L. L., S. H. McArt, A. H. Vaughn, and S. P. Ellner. 2019. Trait-based modeling of multi-host pathogen transmission: plant-pollinator networks. American Naturalist 193:E149–E167.

Tur, C., B. Vigalondo, K. Trøjelsgaard, J. M. Olesen, and A. Traveset. 2014. Downscaling pollen-transport networks to the level of individuals. Journal of Animal Ecology 83:306–317.

Valverde, J., J. M. Gómez, and F. Perfectti. 2016. The temporal dimension in individual-based plant pollination networks. Oikos 125:468–479.

VanderWaal, K. L., and V. O. Ezenwa. 2016. Heterogeneity in pathogen transmission: mechanisms and methodology. Functional Ecology 30:1606–1622.

Vander Zanden, H. B., K. A. Bjorndal, K. J. Reich, and A. B. Bolten. 2010. Individual specialists in a generalist population: results from a long-term stable isotope series. Biology Letters 6:711–714.

Volz, E., and L. A. Meyers. 2007. Susceptible-infected-recovered epidemics in dynamic contact networks. Proceedings of the Royal Society B 274:2925–2933.

White, L. A., J. D. Forester, and M. E. Craft. 2017. Using contact networks to explore mechanisms of parasite transmission in wildlife. Biological Reviews 92:389–409.

———. 2018. Covariation between the physiological and behavioral components of pathogen transmission: host heterogeneity determines epidemic outcomes. Oikos 127:538–552.

Wilber, M. Q., K. M. Pepin, H. Campa III, S. E. Hygnstrom, M. J. Lavelle, T. Xifara, K. C. VerCauteren, and C. T. Webb. 2019. Modelling multi-species and multi-mode contact networks: implications for persistence of bovine tuberculosis at the wildlife-livestock interface. Journal of Applied Ecology 56:1471–1481.

Wilfert, L., G. Long, H. C. Leggett, P. Schmid-Hempel, R. Butlin, S. J. M. Martin, and M. Boots. 2016. Deformed wing virus is a recent global epidemic in honeybees driven by *Varroa* mites. Science 351:594–597.

Woo, K. J., K. H. Elliott, M. Davidson, A. J. Gaston, and G. K. Davoren. 2008. Individual specialization in diet by a generalist marine predator reflects specialization in foraging behaviour. Journal of Animal Ecology 77:1082–1091.

Zhuang, L., N. Cressie, L. Pomeroy, and D. Janies. 2013. Multispecies SIR models from a dynamical Bayesian perspective. Theoretical Ecology 6:457–473.

References Cited Only in the Online Enhancements

Caswell, H. 2008. Perturbation analysis of nonlinear matrix population models. Demographic Research 18:59–116.

———. 2009. Sensitivity analysis: matrix methods in demography and ecology. Demographic Research Monographs. Springer Nature, Cham, Switzerland.

Diekmann, O., H. Heesterbeek, and T. Britton. 2013. Mathematical tools for understanding infectious disease dynamics. Princeton Series in Theoretical and Computational Biology. Princeton University, Princeton, NJ.

Magnus, J. R. 1985. On differentiating eigenvalues and eigenvectors. Econometric Theory 1:179–191.

Associate Editor: Nicole Mideo
Editor: Daniel I. Bolnick

A mining bee (*Andrena* sp.) on a blueberry flower. Photo credit: Scott McArt.